A Ready-to-Use and Storage-Stable Nanofibrous Tissue Patch Fabricated in a Single Step via Reactive Electrospinning

Fei Xu [†], *Megan Dodd* [†], *Heather Sheardown* [†] *and Todd Hoare* * [†]

[†] Department of Chemical Engineering, McMaster University, 1280 Main St W, Hamilton, ON L8S 4L8, Canada

KEYWORDS: Cell electrospinning; Hydrogel; Nanofibers; Cell encapsulation; Tissue scaffolds

ABSTRACT

A reactive electrospinning strategy is used to fabricate viable and proliferative cell-loaded nanofibrous hydrogel scaffolds in a single step using an all-aqueous approach. In situ-gelling and degradable hydrazone-crosslinked poly (oligo ethylene glycol methacrylate)-based hydrogel nanofibrous networks can be produced directly in the presence of cells to support long-term cell viability, adhesion, and proliferation, in contrast to bulk hydrogels of the same composition. Furthermore, the capacity of the gel nanofibers to retain bound water maintains this high cell viability and proliferative capacity following a freeze/thaw cycle without requiring any cryoprotectant additives, ideal properties for ready-to-use functional tissue patches.

INTRODUCTION

Tissue engineering approaches typically aim to mimic the chemical, mechanical, interfacial (i.e. hydrophilicity), and structural properties of native extracellular matrix (ECM) that are known to direct cell responses *in vivo*.[1–4] Hydrogels have attracted significant interest in this context given their low non-specific protein adsorption, cytocompatibility, ease of functionalization, and biomimetic mechanics relative to soft tissues.[5] Multiple types of both bulk[6] and injectable[7] hydrogels have been explored for this purpose with some notable successes, including a range of structured hydrogels with well-defined porosities targeted to support cell spreading and/or growth within the matrix[8–10].

However, significant challenges remain that limit the utility of hydrogel scaffolds for tissue engineering. First, cells tend not to adhere strongly to hydrogels, requiring the incorporation of functional tags such as RGD peptides[11–13] or other cell signalling molecules[10,14] to promote cell interactions with the scaffold. The enhanced substrate-cell contact area achieved in 3D relative to 2D can facilitate sufficient cell adhesion to maintain cell viability even with cell-repellent hydrogel compositions; however, cells encapsulated in such scaffolds typically do not spread or grow, as desired for functional tissue engineering. Second, native ECM contains multiple types of fibrous structures, primarily based on collagen and elastin, on length scales ranging from a few to hundreds of nanometers that provide essential topographical support for cell adhesion and migration[15,16]. While electrospun nanofibrous scaffolds based on "hard" polymers have demonstrated promise due to their capacity to provide such topographical signaling[1,13,17–19], these types of nanofibrous structures are difficult to reproduce in synthetic hydrogel scaffolds more appropriate for engineering soft tissues[2,6,11,15,16]. Third, existing methods to create structured hydrogels (e.g. porogen templating[20], gas foaming[21], emulsification[22], freeze drying[23], stereolithography[24], and

conventional electrospinning[25]) require additives, energy inputs, and/or organic solvents, making these methods either partially or fully incompatible with cells. Consequently, cells must be loaded into such scaffolds post-fabrication, resulting in non-uniform cell distributions and/or challenges in spatial patterning. While 3D bioprinting can in part address these challenges, the resolution of existing 3D bioprinting approaches is insufficient to create the nanoscale topologies particularly useful for cell signaling.[26]

Given that electrospinning has the capacity to create the types of nanofibrous but microporous networks particularly suitable for cell growth, significant effort has been invested in adapting conventional electrospinning processes to include cells, albeit with mixed success. Simply electrospinning polymer fibers on top of plated cells is suitable to create 2D cell scaffolds but cannot create scaffolds in which cells are distributed in 3D.[27] Alternately, coaxial needles in which the cell medium was contained within the core and a polymer solution was extruded as a shell have been reported to encapsulate both mammalian[28] and bacterial cells[29,30] within polymeric microfibers. However, the polymer used for the outer shell must be either water-soluble (in which case the scaffold dissolves when placed in media) or water-insoluble and dissolved in an organic solvent (inducing cytotoxicity during processing and leaving behind a "hard" polymer shell that encapsulates the cells and presents challenges with nutrient transport). Side-by-side simultaneous cell electrospraying and nanofiber electrospinning[31] offers another option for creating 3D cell-loaded scaffolds but requires organic solvents and a fairly complex electrospinning geometry.

Recently, we reported an alternative approach to fabricate hydrogel-based nanofibers via an all-aqueous process based on the concept of reactive electrospinning.[32] Oligomers based on poly(oligoethylene glycol methacrylate) (POEGMA), a poly(ethylene glycol)-mimetic polymer with significantly enhanced chemical and mechanical tunability[33], were functionalized with

hydrazide and aldehyde groups and electrospun from a double barrel syringe. Mixing of the functional oligomers results in rapid *in situ* hydrazone crosslinking to covalently stabilize well-defined nanofibers without requiring any post-crosslinking, organic solvents, or additives. The hydrazone bond is also hydrolytically labile, enabling slow (~12 week) degradation of the scaffold over time[32]. Relative to previously reported methods to electrospun hydrogels[13,34], our approach is unique in that it does not require external energy inputs (e.g. UV irradiation or heating) or any type of templating fiber.

Herein, we apply these unique advantages to directly fabricate uniform cell-loaded nanofibrous scaffolds capable of supporting cell adhesion and growth in 3D in a single step by co-electrospinning cells with our functional oligomer solutions. The topography and hygroscopicity of the resulting nanofibrous hydrogel network facilitate cell responses not observed in conventional (i.e. non-fibrous) hydrogel networks and stabilize cells upon freezing, preserving the capacity of cells to remain viable and proliferate within the scaffolds following cold storage without the need for added cryoprotectants.

EXPERIMENTAL SECTION

Synthesis of POEGMA polymers

Hydrazide-functionalized POEGMA (POH) and aldehyde-functionalized POEGMA (POA) were synthesized by free radical polymerization as previously described.[32] In brief, POH was prepared by adding 2,2-azobisisobutryic acid dimethyl ester (AIBMe, 37 mg, Wako Chemicals), oligo (ethylene glycol) methyl ether methacrylate (OEGMA, 4.0 g, Sigma-Aldrich), acrylic acid (AA, 0.25 g, Sigma-Aldrich) and dioxane (20 mL, Caledon Labs) to a flask and polymerizing at 75 °C for 4 hours under magnetic stirring to form poly(OEGMA-*co*-AA). Following purification

via dialysis (6x6 hr cycles against distilled deionized water), poly(OEGMA-*co*-AA) was functionalized with hydrazide groups via the addition of adipic acid dihydrazide (ADH, 2.65 g, Alfa Aesar) and N'-ethyl-N-(3-dimethylaminopropyl)-carbodiimide (EDC, 1.18 g, Carbosynth, Compton CA) to obtain POH. POA was prepared by adding AIBMe (50 mg), OEGMA (4.0 g), N-(2,2-dimethoxyethyl) methacrylamide (DMEMAm, 0.60 g, synthesized in-house as previously described[33]) and dioxane (20 mL) to a flask and polymerizing at 75 °C for 4 hours under magnetic stirring to form poly(OEGMA-co-DMEMAm). Following purification via dialysis (6x6 hr cycles against distilled deionized water), the poly(OEGMA-co-DMEMAm) polymer was dissolved in 100 mL of 0.25 M HCl to hydrolyze the acetal groups to aldehydes. Both final polymers were purified by dialysis (6x6 hr cycles against distilled deionized water), lyophilized, and stored in sterile 1× PBS at a concentration of 15 wt% at 4 °C for further use. The molar concentrations of functional groups on POH and POA were calculated by ^{1}H-NMR (600 MHz, Bruker) and titration (ManTech automatic titrator, 0.1 M NaOH titrant, 1 mg/mL polymer solution), while the molecular weights of POH and POA were determined by aqueous gel permeation chromatography. See Support Information Table S1 for full characterization data and methodologies for the precursor polymers.

Cell culture

NIH 3T3 fibroblasts (ATCC) and C2C12 myoblasts (ATCC) were cultured in Dulbecco's Modified Eagle's Medium (DMEM, Life Technologies) with 10% fetal bovine serum (FBS, ThermoFisher) and 1% penicillin-streptomycin (ThermoFisher) in a gas plasma-treated polystyrene petri dish (VWR). Both 3T3 fibroblasts and C2C12 myoblasts were cultured to ~80% confluency before use. Non-treated petri dishes (Fisher Scientific) were used to culture both bulk and nanofibrous hydrogel-encapsulated cells to ensure that no driving force was present for cells

to migrate from the scaffolds to adhere on the petri dishes. All cells were incubated at 37°C and 5% CO_2.

Preparation of cell-loaded electrospun nanofibrous hydrogels

Poly (ethylene oxide) (PEO, M_w = 600,000 g/mol, Sigma-Aldrich) was dissolved in sterile DMEM at a concentration of 5 wt%. Subsequently, 0.25 mL of PEO solution was added to 0.25 mL POH or POA solution (both at 15 wt%) to form the POH+PEO and POH+POA precursor electrospinning solutions with a net concentration of 7.5 wt% POH or POA and 2.5 wt% PEO. Cells were added to the POH+PEO precursor solution by centrifuging a 1 mL cell suspension (1×10^6 cells/mL) and suspending the resulting cell pellet in the POH+PEO precursor solution. Subsequently, 0.5 mL of the POH+PEO+cells suspension and 0.5 mL of POA+PEO solution were loaded into separate barrels of a double-barrel syringe equipped with a static mixer (MedMix L series, 2.5 mL capacity). An 18 G blunt needle was connected to the end of the static mixer, and a 10 kV potential difference was applied between the needle and a patterned collector consisting of multiple wires separated by a 1 cm air gap (Glassman High Voltage, 0 to 20kV, 700 μA, 115 V 1PH AC input). A syringe pump was used to pump the precursor solutions at a rate of 10 μL/min for one hour for electrospinning, after which the (dry) scaffold was immediately transferred into the DMEM growth media. Cell-free controls were performed using the same parameters but excluding cells from the POH-PEO precursor solution. The entire protocol was conducted inside a biosafety cabinet to maintain sterility, with the humidity for all experiments maintained between 23-26% RH. The resulting cell densities for 3T3 and C2C12-loaded electrospun hydrogels were 4600 ± 2500 cell/cm^2 and 4200 ± 1300 cells/cm^2 respectively (20 images analyzed per sample).

Preparation of cell-loaded bulk hydrogels

The precursor solutions were prepared as described above for the electrospun scaffolds but omitting the PEO electrospinning aid, resulting in POH and POA concentrations of 15 wt% in the pre-gel solutions; note that the 7.5 wt% solutions as used for electrospinning cannot form bulk gels; gelation is possible with the lower concentrations in electrospinning only because of solvent evaporation during the spinning process to increase the polymer concentration. The same double barrel syringe used for electrospinning experiments was used to extrude hydrogels into a rubber mold of diameter 9 mm and thickness 2 mm, with macroscopic gelation apparent after ~30 minutes. Hydrogels were maintained at room temperature for one hour (to be consistent with the electrospinning protocol) and then transferred into DMEM media and cultured using the same techniques as the electrospun scaffolds.

Mechanical properties of scaffolds

The Microsquisher (CellScale Biomaterials Testing, Waterloo, Canada) was used to measure the elastic properties of electrospun cell-loaded scaffolds. Samples were loaded on the instrument by puncturing them with forks consisting of 5 pins (diameter 254 μm) spaced 7 mm apart. The forks were then attached to a 559 μm gauge cantilever to allow for high-resolution mechanical measurements. Samples were stretched to 10% elongation over at least 15 cycles, using with loading and recovery durations of 20 seconds each and relaxation times of 5 seconds. The thickness of tested samples was ~50 μm. See Support Information Video S1 for a visual description of the testing method.

Microscopic analysis of cell-loaded scaffolds

Scanning electron microscopy (SEM, Tecan Vega II LSU instrument) was used to observe both scaffold and cell morphologies after electrospinning. All SEM images were collected at a voltage of 10 kV using a working distance of 6 mm. SEM samples were prepared by mounting the

electrospun scaffolds on a SEM stub and subsequently sputter coating the scaffolds with gold to prevent charging. Confocal laser scanning microscopy (CLSM, Nikon) and fluorescence microscopy (FL, Axiovert 200, Carl Zeiss) were used to track cell live/dead responses, the proliferation of cells within the scaffolds, and cell morphologies after fluorescence staining using excitation wavelengths described in the following sections relevant to each assay conducted. Bright field (BF) images were also collected to correlate the cell location with the fibrous network. Confocal z-stack images (3D view) were collected by scanning planes at 10 μm intervals (the approximate diameter of the cells used) from the bottom to the top of the electrospun scaffold, using the same imaging parameters as used to collect the 2D images for each plane. For cell proliferation tracking, all parameters such as the voltage, offset, and gain were kept the same from day 1 to day 18, allowing for accurate tracking of the fluorescence emitted per cell in the CFSE assay.

CFSE staining for cell tracking

Carboxyfluorescein diacetate succinimidyl ester (CellTrace^{TM} CFSE, ThermoFisher) was used to label cells to track proliferation and assess morphology. For proliferation assays from fresh samples and to assess the distribution of cells within the electrospun scaffolds, 3T3 or C2C12 cells were pre-stained with CFSE stock as per the manufacturer's protocol and then electrospun as described previously. For freeze-thaw proliferation assays, pre-encapsulated 3T3 cells were stained one day following the thawing of the scaffold, again using the same protocol but adding 4 x 3 mL washes in PBS to ensure any stain not taken up by cells is removed from the hydrogel scaffold. For cell morphology assays, pre-loaded 3T3 or C2C12 were stained with CFSE (using the recommended protocol with the additional washes) on the day the morphology assessment was

conducted (i.e. following either 1, 5, 7 and 18 days of cell culture). In this latter assay, paraformaldehyde stock (PFA, Sigma-Aldrich, 3 wt%) was used to fix the cells prior to imaging.

Far Red staining for cell tracking

In addition to CFSE, Far red (CellTrace^{TM} CFSE, ThermoFisher) was used to label cells to track proliferation within the freeze-thawed cell-loaded scaffolds. Cells were stained with Far Red stock solution following the manufacturer's protocol at the first day after thawing, after which the same imaging procedure as outlined for CFSE tracking was conducted.

Rhodamine 123 labeling of POA

Rhodamine 123 (Sigma Aldrich) was used to label the POA precursor polymer to enable imaging of the polymer distribution within the nanofibrous electrospun hydrogels in the dry and swollen states. Rhodamine 123 (5 mg) was mixed with POA precursor solution (1 g, 15 wt% in deionized water) for 24 hours under magnetic stirring to form a Schiff base that was subsequently reduced to a stable secondary amine linkage via the addition of sodium cyanoborohydride (8.25 mg, 10 mol eq. to rhodamine 123, 48 hours under stirring). The resulting labeled polymer was purified via dialysis (6x6 hr cycles against distilled deionized water), with the final rhodamine 123-labeled POA product lyophilized and stored in a 15 wt% solution in 1x PBS at 4 °C.

Cell viability assays

Cytotoxicity of polymer precursors For assessing the cytotoxicity of the polymer precursors, 3T3 fibroblasts or C2C12 myoblasts were seeded in a 96 well plate at a density of 10,000 cells per well and incubated in 100 μL DMEM at 37°C and 5% CO_2 for 24 hours. The plate was then washed with PBS and the growth medium replaced with 100 μL of DMEM containing POH, POA, and/or PEO, at concentrations ranging from 1 to 2 mg /mL, with cells then incubated for an additional 24 hours. Subsequently, the medium (with the materials) was removed and replaced with 90 μL of

fresh DMEM and 10 μL of PrestoBlue reagent (ThermoFisher), followed by an additional one hour incubation step at 37°C. Cell viabilities were estimated using a plate reader (Infinite M200 Pro, Tecan) to measure fluorescence (560 nm excitation/ 590 nm emission), with the result normalized to a cell-only (non-treated) control. Cell viabilities in the polymer precursor solutions used for electrospinning (7.5 wt% of POH/POA, 2.5 wt% of PEO) following the same method.

Cell viabilities during electrospinning For assessing cell viability as a function of applied voltage during electrospinning, a cell suspension of 100,000 cells/mL in DMEM media was processed at voltages of 0, 5, 10 and 15 kV using the same setup used for hydrogel scaffolds but increasing the feed rate to 200 μL/min (1 cm falling distance) and using a 60 mm × 15 mm petri dish petri dish as the collector to ensure all cells were collected. Following, the cells were aliquoted into separate wells of a 96 well plate, with each well containing 10,000 cells in 100 μL DMEM. Cells were cultured at 37°C for 24 hours before assessing viability using the same PrestoBlue protocol outlined above. For assessing cell viability as a function of dehydration time, cells were seeded in a 96 well plate at a density of 10,000 cells per well in 100 μL DMEM at 37°C for 24 hours. Following, the DMEM was removed and the plate was left in the incubator for defined times. Cell viability following different media-free exposure times was then assessed using the same PrestoBlue protocol outlined previously. For assessing cell viability as a function of cell stress during electrospinning, a cell suspension of 1,000,000 cells/mL was centrifuged and the cell media was replaced PEO (600 kDa) dissolved in PBS at different concentrations (1 wt%, 2 wt% and 3 wt%). The cell suspension in PEO was then loaded in a 3 mL syringe and electrospun into a 60 mm × 15 mm petri dish at voltages of 0, 5, 10, and 15 kV using feed rate of 200 μL/min and a 1 cm falling distance. The (liquid) product was then transferred into a 96 well plate at a

concentration of 10,000 cells/well in 100 μL of DMEM+PEO solution. Cells were cultured at 37°C for 24 hours before assessing viability using the same PrestoBlue protocol outlined above.

Live/dead assay For assessing cell viability within the electrospun nanofibrous hydrogels and the conventional bulk hydrogels, a calcein AM/ethidium homodimer-1 (Et-D) LIVE/DEAD assay (ThermoFisher) was used following the manufacturer's protocol except using longer incubation time (~1.5 h) at room temperature to allow the dyes to fully penetrate into the gel phase and an additional 4 x 3 mL PBS washes to ensure any non-bound dye was fully removed from the gel scaffold.

Frozen cell-matrix preparation 3T3 cell-loaded nanofibrous hydrogels were produced via electrospinning as previously described. After 1 h of electrospinning, the electrospun matrix was immediately immersed in liquid nitrogen (-195°C) without adding any additional cryoprotectants and left frozen in liquid nitrogen for 3 weeks. Following, the frozen scaffold was placed in pre-heated 37°C DMEM growth media (with 10 % FBS and 1% PS) to thaw and then, without any further purification steps, placed in an incubator and cultured over times ranging from 1 to 18 days. Cell viability (LIVE/DEAD assay) and proliferation (CFSE assay) were assessed as previously described for the fresh scaffolds.

RESULTS AND DISCUSSION

Cell viability following electrospinning

POEGMA-hydrazide (POH) and POEGMA-aldehyde (POA) were synthesized by free radical polymerization as previously described[32] (Support Information Table S1), with neither precursor polymers exhibiting significant cytotoxicity to either 3T3 mouse fibroblasts or C2C12 mouse myoblast cells used herein as proof-of-concept cells (Support Information Figure S1a-b).

Nanofiber precursor solutions were then prepared consisting of 7.5 wt% POH/POA and 2.5 wt% poly(ethylene oxide) (PEO, M_w=600,000 g/mol) in a sterile mixture of 1:1 phosphate buffered saline (PBS) and DMEM cell medium; PEO was added as an electrospinning aid to ensure sufficient chain entanglement to create nanofibers[32]. 3T3 or C2C12 cells (10^6 cells/mL) were suspended in the POH+PEO precursor solution, after which both precursor solutions were loaded into a double barrel syringe equipped with a static mixer (to ensure intimate mixing between the precursor polymers) and electrospun onto a stationary parallel electrode collector (Figure 1A). Both 3T3 and C2C12 cells also maintained high viabilities when exposed to the nanofiber precursor solutions (Support Information Figure S1c). Electrospinning 3T3 and C2C12 cells alone under high voltage resulted in very high cell viability (91% for 3T3 and 98% for C2C12 at 15 kV, Support Information Figure S1d), consistent with previous reports that indicated minimal cell death due to the low (~700 mA) current used for electrospinning[35]. Furthermore, despite the fact that scaffolds were collected "dry", cells electrospun without any scaffolding materials maintained high viabilities after 1 h in dehydrated conditions at 37 °C (91% for 3T3 and 83% for C2C12, Support Information Figure S1e). The high hygroscopicity of the gel scaffold would significantly prolong this viability when cells are co-electrospun with the scaffolding materials, although all scaffolds were still collected after 1 h of electrospinning since this time is sufficient to allow for the fabrication of a uniform self-supported cell-loaded patch. This processing time is orders of magnitude faster than typical approaches reported, which commonly require hours/days long solvent extraction/porogen removal and diffusive post-loading of cells. Similarly, when cells were electrospun in PEO-only solutions, the viscosity of which (Support Information Table S2) can induce additional shear stresses on the cells during the fiber stretching process[36], high cell viabilities were again achieved provided voltages did not exceed 10 kV (Support Information

Figure S1f-g). As such, neither the polymer precursors nor the electrospinning process significantly impacted cell viability.

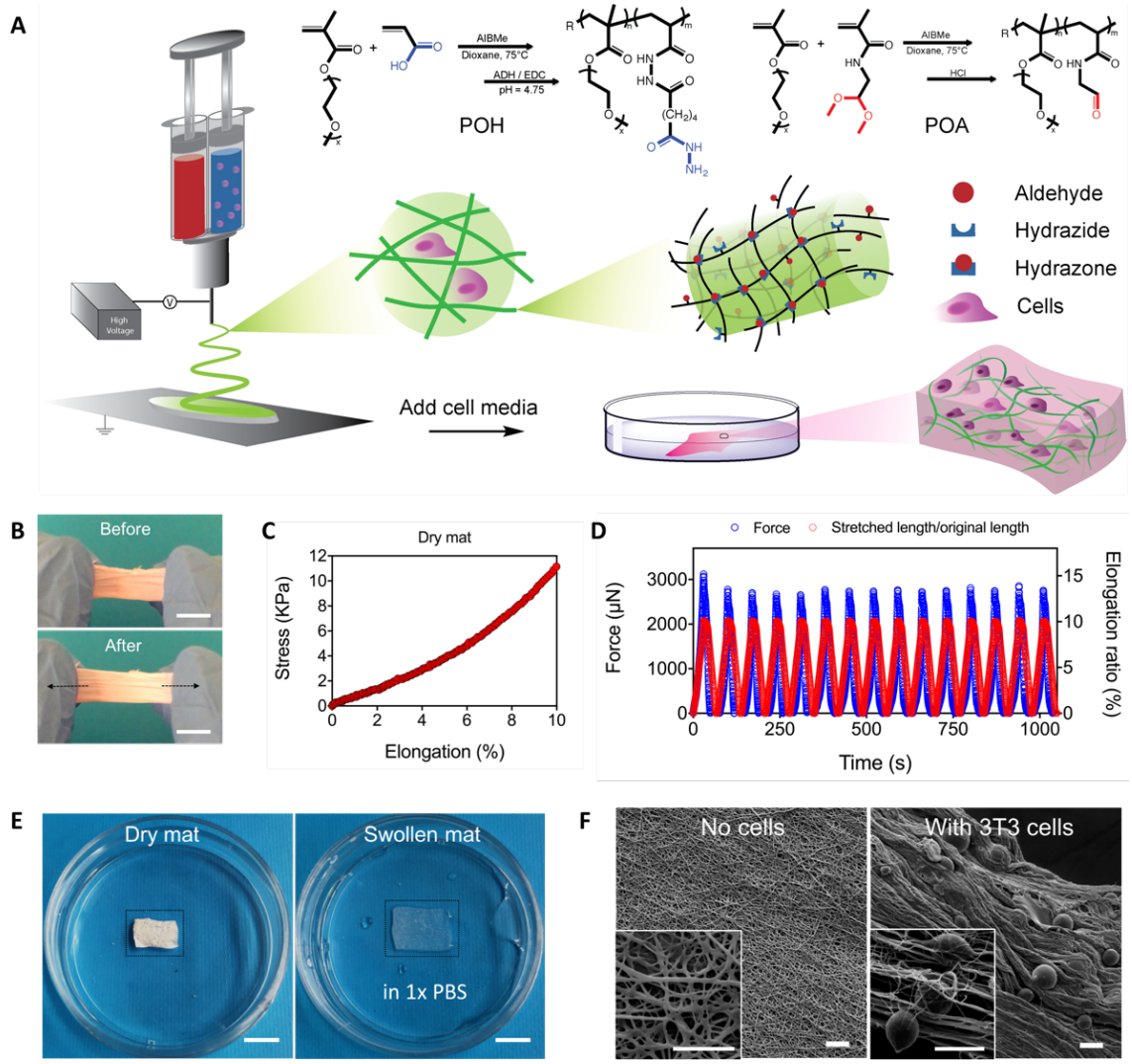

Figure 1. Reactive electrospinning can fabricate mechanically strong cell-loaded nanofibrous hydrogel scaffolds. (A) Schematic diagram demonstrating the reactive cell electrospinning process for cell encapsulation in nanofibrous hydrogels in a single, all-aqueous step. (B) Cell-loaded POEGMA electrospun scaffolds before and after manual stretch. Scale bars = 1 cm. (C) Stress-strain curve of a dry cell-loaded electrospun mat. (D) Cyclic tensile test of dry cell-loaded scaffold (10% elongation, 15 cycles) demonstrating the elasticity of the dry scaffolds. (E) Electrospun scaffold containing cells before and after swelling in 1× PBS. Scale bars = 1 cm. (F) SEM images of POEGMA nanofibers electrospun with and without 3T3 cells. Scale bars = 20 μm.

Mechanical and morphological properties of cell-loaded scaffolds

The electrospun cell-loaded scaffold was easy to handle and could be physically stretched without breaking (Figure 1B and Support Information Video S1), with a dry tensile modulus of ~100 kPa. (Figure 1C). Repeated tensile cycling at 10% elongation indicated the highly elastic properties of the scaffold in the dry state (Figure 1D and Support Information Video S1). The hydrogel nanofibers reswelled within one minute when immersed back into DMEM or PBS to form a nearly transparent matrix that maintained stability and shape over ~30 days of incubation time (Figure 1E and Support Information Video S1); in contrast, PEO-only electrospun scaffolds without the gelling POEGMA component dissolved fully within seconds.[32] The presence of cells during the electrospinning process slightly increased the average nanofiber diameter from 0.4 ± 0.1 μm in the absence of cells to 0.8 ± 0.2 μm (with 3T3 cells) or 0.7 ± 0.3 μm (with C2C12 cells) (Figure 1F and Support Information Table S3). This result is consistent with the applied voltage being less effectively stretching the nanofibers during the electrospinning process in the presence of large and elastic cells, although the nanoscale fiber dimensions are maintained. The nanofibrous scaffold structure was maintained following swelling (Figure 2A-B), with the swollen fiber diameter of 2.2 ± 0.2 μm significantly smaller than achieved by even the best existing 3D printing processes (Support Information Figure S2).

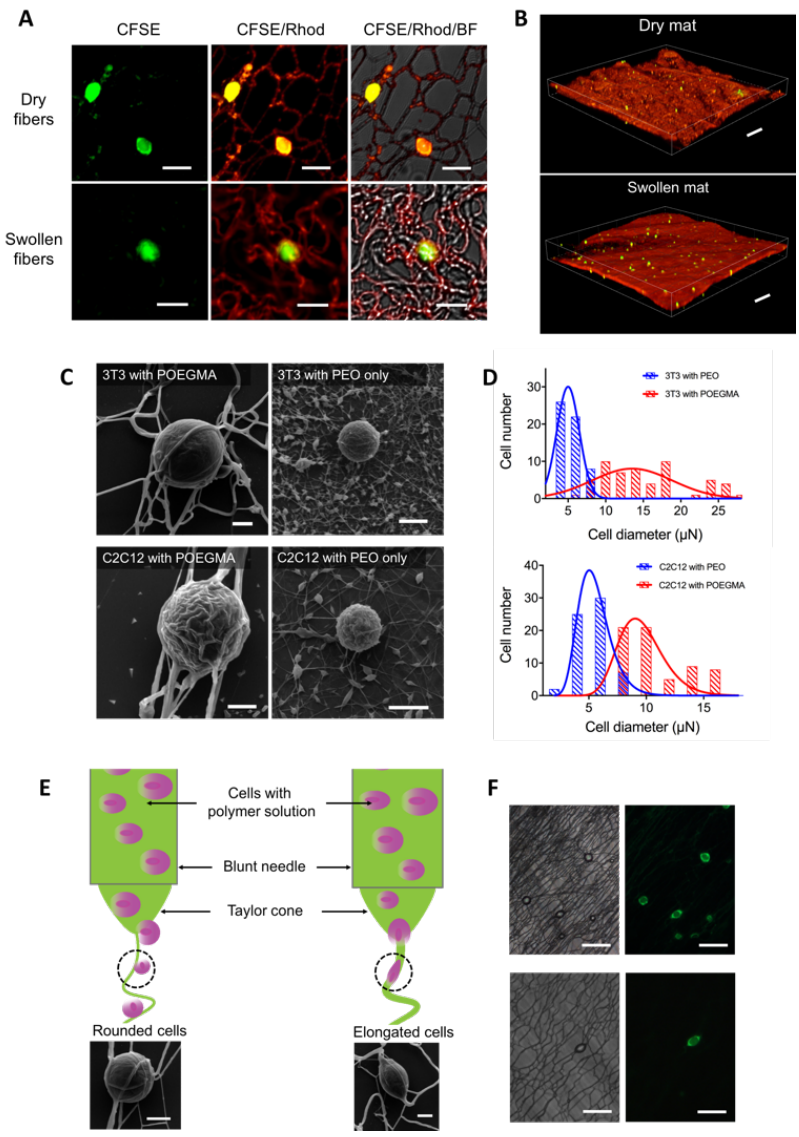

Figure 2. Electrospun cells can remain hydrated and assume different morphologies within nanofibrous hydrogel scaffolds. (A) Confocal images of 3T3 cells pre-stained with CFDA-SE (CFSE, green) and POEGMA electrospun nanofibers pre-stained with Rhodamine 123 (Rhod, red) imaged in fluorescence mode (488 nm and 563 nm excitation) and bright field (BF) mode in the dry and swollen states. Scale bar = 20 μm. (B) 3D confocal reconstructions of the nanofiber and cell distributions of dry (top) and swollen (bottom) scaffolds. Scale bars = 200 μm. (C) SEM images of 3T3 fibroblasts and C2C12 myoblasts electrospun within POEGMA hydrogel nanofibers and PEO fibers. Scale bars = 5 μm. (D) Cell diameter distributions of 3T3 fibroblasts (n=56) and C2C12 myoblasts (n=64) electrospun within POEGMA hydrogel nanofibers and PEO fibers. (E) Proposed mechanism for the formation of rounded and elongated cells depending on the position of the cells relative to the Taylor cone during electrospinning. Scale bars = 5 μm. (F) Bright field and fluorescence microscope images of 3T3 cells pre-stained with CFDA-SE show cells with both rounded (entrapped) and elongated (encapsulated) morphologies; the correspondence of the cell positioning between the light field images and the CFSE-stained fluorescence images confirm the identity of the cells in each image. Scale bars = 50 μm. All electrospun POEGMA nanofibers were prepared using 7.5 wt% POH/POA mixed with 2.5 wt% PEO; PEO-only fibers were prepared with 2.5 wt% PEO only (10 kV, 1 h).

Morphologies of encapsulated cells

SEM images of cells within the nanofibrous scaffolds (i.e. dried and under vacuum) exhibited cell average diameters of 15 ± 6 μm for 3T3 and 10 ± 3 μm for C2C12, identical to the diameters of fresh cells in DMEM suspension (14 ± 2 μm for 3T3 and 12 ± 2 μm for C2C12); in contrast, cells electrospun in a PEO-only matrix were significantly smaller (5 ± 2 μm for 3T3 and 6 ± 2 μm for C2C12) (Figure 2C-D and Support Information Table S3). This result demonstrates the unique capacity of the hydrogel scaffold to bind water and thus supporting a hydrated environment around the cells even when the scaffold is macroscopically dry, allowing cells to maintain their morphology even in a vacuum.

Two clearly distinct cell morphologies are evident for both 3T3 and C2C12 electrospun cell scaffolds (Figure 2E-F and Support Information Figure S3). The majority of cells (~90% in both scaffold types, as per image analysis) were rounded and appear to be physically entrapped *between* a web of nanofibers (Figure 2E) and/or surrounded by sheaths of nanofibers when thicker scaffolds were prepared (Support Information Figure S3a-b). However, a significant sub-population of cells (~10% in both scaffold types) appeared significantly elongated and encapsulated *within* nanofibers (Figure 2E), with both the position of the cells and direction of elongation corresponding directly to that of a single or a few aligned nanofibers (Support Information Figure S3c-d). This result is consistent with statistical probabilities of cells streaming *beside* the Taylor cone (i.e. nanofibers form independently to entrap cells *between* fibers) or *within* the Taylor cone (i.e. a gel sheath forms directly *around* cells) during the electrospinning process.

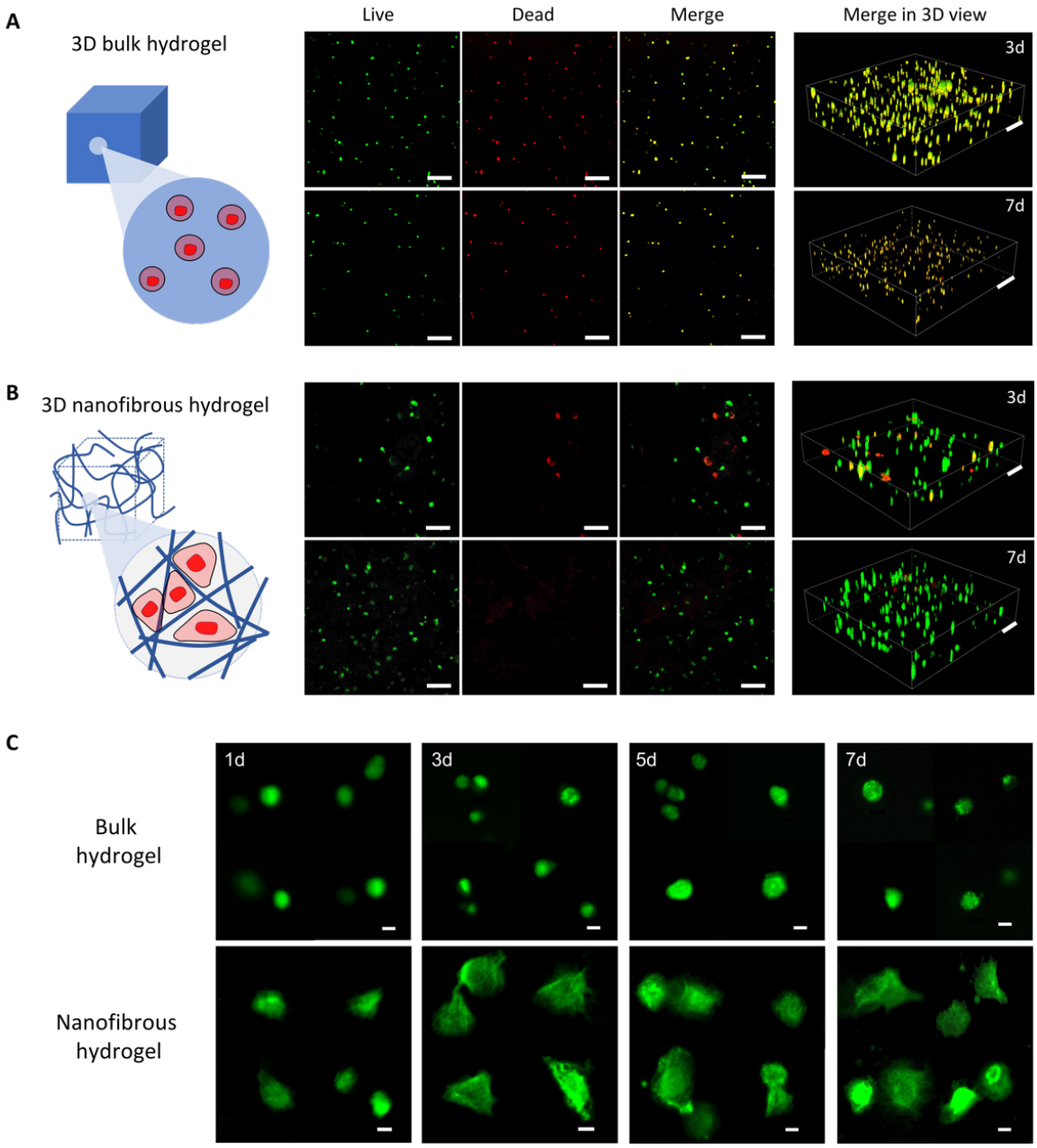

Figure 3. Electrospun nanofibrous hydrogels can maintain significantly higher cell viabilities and uniquely support cell-matrix interactions relative to bulk hydrogels of the same composition. (A-B) Confocal images of 3T3 cells encapsulated in (A) bulk hydrogels or (B) electrospun nanofibrous hydrogels of the same chemical composition after 3 days and 7 days of incubation showing live cells (green, 488 nm), dead cells (red, 561 nm), the overlay between the green and red channels, and 3D images showing the distribution of cells throughout the scaffold volume. Scale bars = 200 μm. (C) Comparison of cell morphology of 3T3 cells within bulk and nanofibrous hydrogels of the same chemical composition following 1, 3, 5, and 7 days of incubation (n=4). Scale bars = 10 μm. Cell density = 1×10^6 cells/mL in all cases. 3T3 cells were post-stained using CFDA-SE and fixed using PFA prior to imaging.

Cell viability in nanofibrous hydrogel scaffolds

To investigate the viability of cells within the electrospun scaffolds, a calcein AM/ethidium homodimer-1 LIVE/DEAD stain was used to characterize cells within the scaffolds 3 and 7 days post-electrospinning (Figure 3A-B; see Support Information Figure S4 for C2C12 results). Significantly more live cells (green) and fewer dead cells (red) were observed after 3 days of incubation in the electrospun hydrogel scaffolds compared to bulk hydrogels of an identical chemical composition. Furthermore, in the bulk hydrogels, cells staining as green (alive) tended also to stain red, indicative of apoptotic cells[37] (yellow in the composite image, Figure 3A); such cells are not evident in the electrospun nanofibrous gel (Figure 3B). This difference becomes even more distinct after 7 days, with 3D confocal microscopy images demonstrating that an increasing percentage of the cells in the nanofibrous hydrogels remained viable (suggestive of proliferation of live cells inside the matrix) while only apoptotic or dead cells were found in the bulk hydrogels (Figure 3 and Support Information Figure S4). Interestingly, this viability difference is observed even though the bulk hydrogels were never dried (i.e. they were extruded and *in situ*-gelled all in the hydrated state) while the electrospun scaffolds were macroscopically dry during the fabrication process, a processing difference that would in most cases result in significantly lower cell viability in the dried (electrospun) scaffolds but here shows the opposite. This difference in cell viability is matched by a clear difference in cell shape, with cells entrapped within the bulk hydrogel remaining spherical and small over the full seven-day assay while cells in the electrospun nanofibrous hydrogel appearing both larger and more asymmetric in shape, the latter consistent with the formation of adhesions with the cell scaffold (Figure 3C). Note that plating cells on top of the same POEGMA hydrogel in 2D results in almost complete suppression of cell adhesion[38], consistent with the high hydrophilicity of POEGMA-based hydrogels previously reported[39]. As

such, the nanofibrous morphology significantly enhances the capacity of cells to interact with the matrix and thus remain viable over extended periods, although the role of the nanofibrous scaffold in enhancing for nutrient/waste transport is likely also to contribute to the improved cell viability observed.

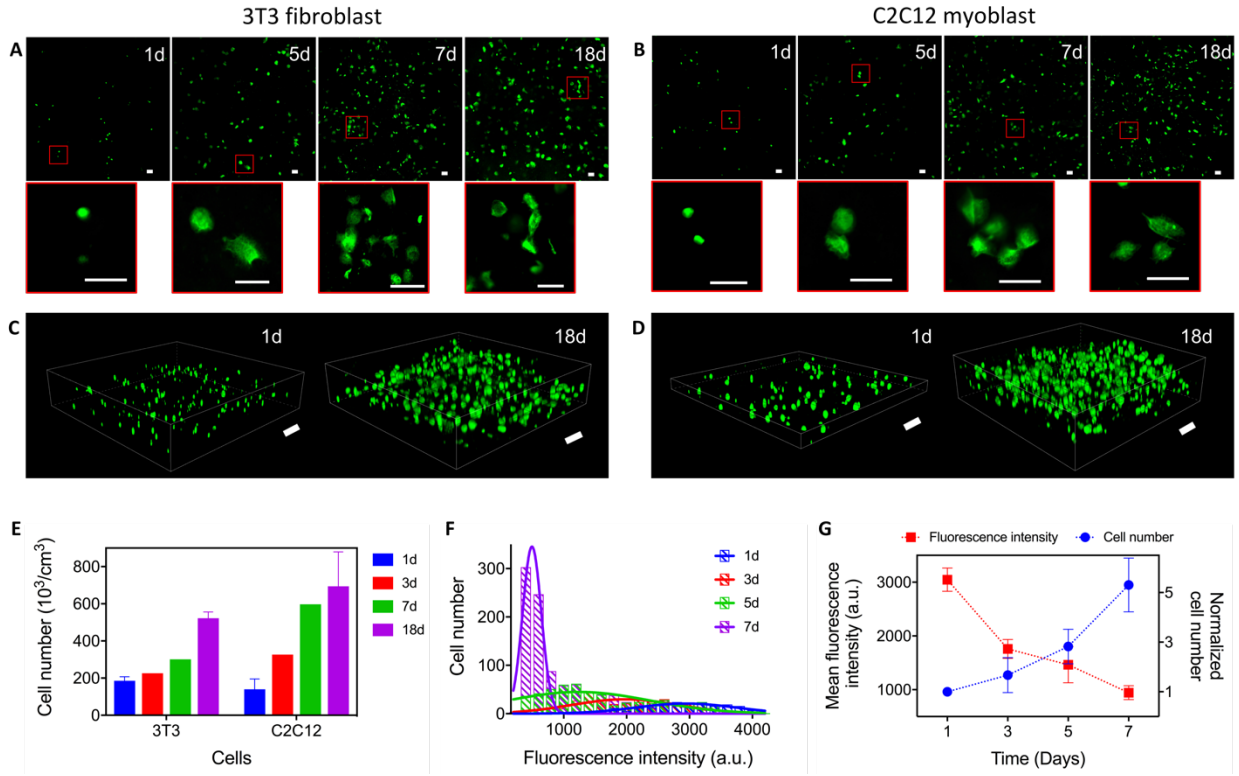

Figure 4. Cells can proliferate and spread within electrospun nanofibrous hydrogels. (A-B) Confocal fluorescence microscopy images of 3T3 (A) and C2C12 (B) cells after 1, 5, 7 and 18 days of cell culture demonstrating increasing cell number over time; subset images show the concurrent changes in cell morphology as a function of culture time. Scale bars = 50 μm. (C-D) 3D confocal microscopy images of 3T3 (C) and C2C12 (D) cells encapsulated in POEGMA hydrogel nanofibers after 1 day and 18 days. Scale bars = 200 μm. All cells were post-stained using CFDA-SE (488 nm, green) and fixed using 3 wt% PFA prior to imaging. (E) Volumetric 3T3 and C2C12 cell densities measured via ImageJ analysis of 3D confocal microscopy images in Figure 4C-D as a function of culture time, confirming cell proliferation within the electrospun scaffolds. All cells were post-stained using CFDA-SE and fixed using PFA prior to imaging (n=3 images per sample). (F) Histogram of 3T3 cell number versus fluorescence intensity per cell of 3T3 cells at 1, 3, 5 and 7 days calculated via CFDA-SE staining and the 2D confocal microscopy images in Support Information Figure S5c (n=4, 2 images per sample for analysis). (G) Mean fluorescence intensities and normalized 3T3 cell numbers at 1, 3, 5 and 7 days culture times from (e) (n=4, 4 images per sample for calculation). Cell density = 1×10^6 cells/mL.

Cell proliferation in nanofibrous hydrogel scaffolds

Cell proliferation within the nanofibrous hydrogel scaffolds was subsequently tracked via long-term (18 day) incubation of the cell-loaded scaffolds in growth media. Both 3T3 and C2C12 cells proliferate within the electrospun hydrogel scaffolds in all three dimensions, with 3D confocal microscopy images indicating that cells uniformly fill the full volume of the nanofibrous hydrogel scaffold (Figure 4A-D, Support Information Figure S5a-b). Image analysis of the 3D confocal microscopy images suggest a ~4-fold increase in cell density for C2C12 cells and a ~3-fold increase in cell density for 3T3 cells between day 1 and day 18 of cell culture (Figure 4E). A simultaneous increase in cell number and decrease in fluorescence intensity per cell were also observed for each cell type using the CFSE assay tracking 2D sections of the scaffolds as a function of time (Figure 4F-G and Support Information Figure S5c), confirming that the increase in cell number is a result of the proliferation of live encapsulated cells as a parent cell splits its fluorescence between two daughter cells. Proliferation was not observed when either 3T3 or C2C12 cells were plated on a non-treated petri dish (i.e. no cell adhesion), while a similar degree of cell proliferation was observed between the 3D nanofibrous hydrogel and cells plated directly on a treated (i.e. adhesive) 2D petri dish assay (Support Information Figure S6). Coupled with the clear asymmetrical cell morphologies observed at incubation times of 5 days and later within the nanofibrous hydrogel networks (Figure 4), these results confirm that electrospun gel scaffolds can support cell-scaffold interactions and subsequent proliferation within the scaffold.

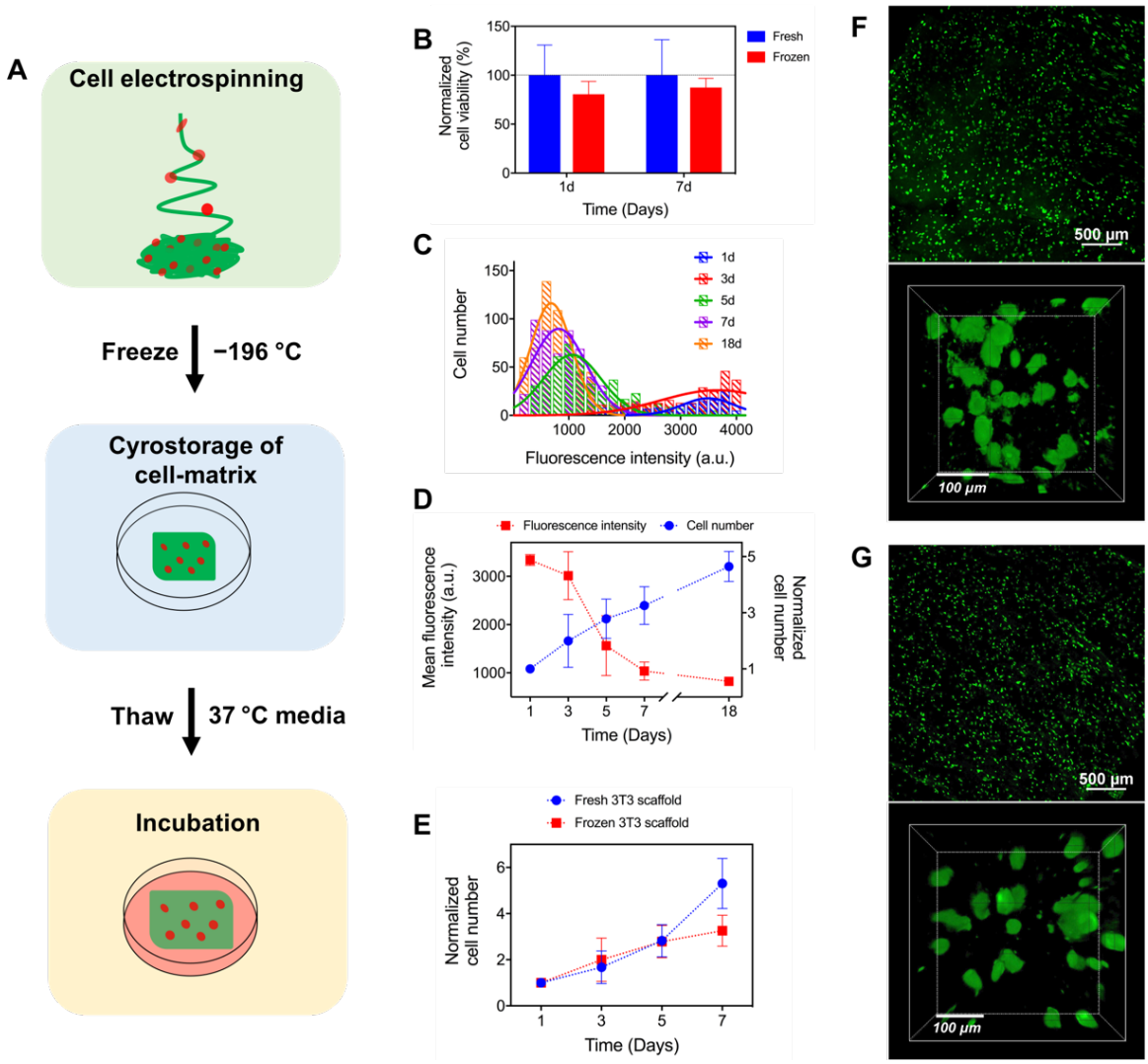

Figure 5. Electrospun nanofibrous hydrogels can maintain cell viability and cell proliferative ability after a freeze/thaw cycle without additional cryoprotectants. (A) Schematic of the process to prepare, freeze, and thaw an electrospun tissue patch. (B) Comparison of normalized cell viabilities of fresh and frozen 3T3 cells loaded in POEGMA electrospun scaffolds confirming that the nanofibrous scaffolds could protect cells during freezing. (n=4, calculated from 3D confocal images). (C) Histogram of 3T3 cell number versus fluorescence intensity per cell of 3T3 cells following a freeze/thaw cycle after 1,3, 5, 7 and 18 day culture times, calculated from confocal images (Support Information Figure S8a) using CFDA-SE staining (n=4, 2 images per sample for analysis). (D) Mean fluorescence intensities and normalized 3T3 cell number following a freeze/thaw cycle after 1, 3, 5, 7, and 18 day culture times (n=4, 3 images per sample for calculation). (n=4, 4 images per sample for calculation). (E) Comparison of proliferation of 3T3 cells with and without freezing at 1, 3, 5 and 7 days calculated from 2D confocal images using CFDA-SE staining. (F-G) Confocal microscopy of 3T3 cells within fresh (F) and frozen (G) POEGMA nanofibrous scaffolds captured by 2D (top) and 3D (bottom) images after 18 day culture. Cell density = 1×10^6 cells/mL in all cases. 3T3 cells were post-stained using CFDA-SE and fixed using PFA prior to imaging.

Storage-stable tissue patches following a freeze/thaw cycle

Given the capacity of the scaffold to bind water and promote cell adhesion/proliferation, the potential of reactive cell electrospinning to create ready-to-use tissue patches that could be frozen, thawed, and used as needed by a patient was next assessed. Electrospun 3T3 cell scaffolds were quick frozen in liquid nitrogen immediately after the 1 hour electrospinning experiment, stored frozen for 14 days in liquid nitrogen, thawed in pre-warmed DMEM at 37 °C, and then cultured identically to the fresh scaffolds (Figure 5A). High cell viability was maintained within the scaffold after the freeze/thaw process despite the fact that no cryoprotectants were used, with 80% viability after 1 day and 87% after 7 days compared to a fresh scaffold (Figure 5B). A similar clear increase in the number and percentage of viable cells was observed via live/dead assay results (Support Information Figure S7a). Cell shape changed from rounded immediately after thawing to irregular at day 18 (Support Information Figure S7b), consistent with the capacity of cells to adhere to the matrix (as observed with fresh scaffolds, Figure 3C). Furthermore, the proliferative capacity of 3T3 cells within the 3D electrospun matrix was maintained even after freezing and cryostorage (Support Information Figure S7c), with both CFSE (Figure 5C-D) and Far Red (Support Information Figure S8) assays indicating the same concurrent increase in cell density and decrease in fluorescence intensity per cell between day 1 and day 18 consistent with cell division events. Indeed, very similar rates of cell proliferation were observed within the fresh and frozen/thawed scaffolds without any apparent lag period in cell proliferation as is often observed following conventional cryostorage (Figure 5E, F-G and Support Information Video S2), suggesting minimal if any cell stress as a result of the freeze/thaw process; we expect that the absence of a required cryoprotectant eliminates the induction period. Together, these observations suggest that the electrospun scaffolds can themselves serve as a cryoprotectant for cells without

the need for the additives or step-wise freezing protocols.[40–42] We attribute this result to the combination of the macroscopic drying of the scaffold during electrospinning (leaving minimal non-bound water to freeze) and the capacity of the hydrogel nanofibers to bind water and thus prevent large-scale ice crystal formation[43,44]. In this manner, reactive hydrogel cell electrospinning allows for one-step fabrication of a functional cell-loaded tissue patch that can be stored between fabrication and use, a significant potential benefit in terms of translating cellularized scaffolds to the clinic.

CONCLUSIONS

In summary, we have demonstrated that reactive electrospinning of hydrazone-crosslinkable POEGMA polymer precursors can create cellularized nanofibrous hydrogel scaffolds in a single and rapid all-aqueous processing step by simply adding cells to one of the precursor polymer solutions. Cells maintain both high viability as well as proliferative capacity following fabrication, in contrast to conventional bulk hydrogels of the same composition. In addition, the capacity of the hydrogel nanofibers to retain bound water both prevents dehydration (and thus cell death) during electrospinning and maintains cell viability and proliferative capacity following a freeze/store/thaw cycle. Together, these properties offering the possibility of creating ready-to-use cellularized tissue patches that can be stored and used immediately as required in therapeutic applications without requiring any purification or additional scaffold preparation steps at the point of care, in contrast to other existing cellularized scaffolds.

ASSOCIATED CONTENT

Supporting Information

The Supporting Information is available free of charge on the ACS Publications website at DOI: 10.1021/acs.biomac.xxxxx.

Additional data on polymer characterizations (chemical properties, viscosity, cell diameters); cell viabilities within polymer precursors and electrospinning conditions (high voltage, dehydration, PEO concentrations); morphologies of cell-loaded scaffolds (bright field images and SEM for 3T3 fibroblasts and C2C12 myoblasts); live/dead assay for C2C12 cells; 3D confocal images of 3T3 and C2C12 cells; analysis of mean fluorescence intensity of 3T3 cells to track cell proliferations. (PDF)

Mechanical properties of cell-loaded scaffolds in dry and wet state. (Video S1, MP4)

Confocal images of cell encapsulations in fresh scaffold and frozen scaffold. (Video S2, MP4)

AUTHOR INFORMATION

Corresponding Author

*Email: hoaretr@mcmaster.ca

ACKNOWLEDGMENT

Funding from the Natural Sciences and Engineering Research Council of Canada (NSERC, Discovery Grant RGPIN 356609 and Strategic Project Grant SPG-447372-13) is gratefully

acknowledged. The authors would like to thank Dr. Harald Stöver for access to a confocal microscope.

REFERENCES

(1) Dvir, T.; Timko, B. P.; Kohane, D. S.; Langer, R. Nanotechnological Strategies for Engineering Complex Tissues. *Nat. Nanotechnol.* **2011**, *6* (1), 13–22.

(2) Stevens, M. M.; George, J. H. Exploring and Engineering the Cell Surface Interface. *Science* **2005**, *310* (November), 1135–1138.

(3) Watt, F. M.; Huck, W. T. S. Role of the Extracellular Matrix in Regulating Stem Cell Fate. *Nat. Rev. Mol. Cell Biol.* **2013**, *14* (8), 467–473.

(4) Place, E. S.; Evans, N. D.; Stevens, M. M. Complexity in Biomaterials for Tissue Engineering. *Nat. Mater.* **2009**, *8* (6), 457–470.

(5) Drury, J. L.; Mooney, D. J. Hydrogels for Tissue Engineering: Scaffold Design Variables and Applications. *Biomaterials* **2003**, *24* (24), 4337–4351.

(6) Benoit, D. S. W.; Schwartz, M. P.; Durney, A. R.; Anseth, K. S. Small Functional Groups for Controlled Differentiation of Hydrogel-Encapsulated Human Mesenchymal Stem Cells. *Nat. Mater.* **2008**, *7* (10), 816–823.

(7) Zhang, J.; Muirhead, B.; Dodd, M.; Liu, L.; Xu, F.; Mangiacotte, N.; Hoare, T.; Sheardown, H. An Injectable Hydrogel Prepared Using a PEG/Vitamin E Copolymer Facilitating Aqueous-Driven Gelation. *Biomacromolecules* **2016**, *17* (11), 3648–3658.

(8) Hwang, C. M.; Sant, S.; Masaeli, M.; Kachouie, N. N.; Zamanian, B.; Lee, S.-H.; Khademhosseini, A. Fabrication of Three-Dimensional Porous Cell-Laden Hydrogel for Tissue Engineering. *Biofabrication* **2010**, *2* (3), 35003.

(9) Lee, T. T.; García, J. R.; Paez, J. I.; Singh, A.; Phelps, E. A.; Weis, S.; Shafiq, Z.; Shekaran, A.; del Campo, A.; García, A. J. Light-Triggered in Vivo Activation of Adhesive Peptides Regulates Cell Adhesion, Inflammation and Vascularization of Biomaterials. *Nat Mater* **2015**, *14* (3), 352–360.

(10) Khalili, A. A.; Ahmad, M. R. A Review of Cell Adhesion Studies for Biomedical and Biological Applications. *Int. J. Mol. Sci.* **2015**, *16* (8), 18149–18184.

(11) Baker, B. M.; Chen, C. S. Deconstructing the Third Dimension - How 3D Culture Microenvironments Alter Cellular Cues. *J. Cell Sci.* **2012**, *125* (13), 3015–3024.

(12) Burdick, J. A.; Anseth, K. S. Photoencapsulation of Osteoblasts in Injectable RGD-Modified PEG Hydrogels for Bone Tissue Engineering. *Biomaterials* **2002**, *23* (22), 4315–4323.

(13) Baker, B. M.; Trappmann, B.; Wang, W. Y.; Sakar, M. S.; Kim, I. L.; Shenoy, V. B.; Burdick, J. a.; Chen, C. S. Cell-Mediated Fibre Recruitment Drives Extracellular Matrix Mechanosensing in Engineered Fibrillar Microenvironments. *Nat. Mater.* **2015**, *14* (12), 1262–1268.

(14) Vega, S. L.; Kwon, M.; Mauck, R. L.; Burdick, J. A. Single Cell Imaging to Probe Mesenchymal Stem Cell N-Cadherin Mediated Signaling within Hydrogels. *Ann. Biomed. Eng.* **2016**, *44* (6), 1921–1930.

(15) Blow, N. Cell Culture: Building a Better Matrix. *Nat. Methods* **2009**, *6* (8), 619–622.

(16) Watt, F. M.; Huck, W. T. S. Role of the Extracellular Matrix in Regulating Stem Cell Fate. *Nat Rev Mol Cell Biol* **2013**, *14* (8), 467–473.

(17) Feiner, R.; Engel, L.; Fleischer, S.; Malki, M.; Gal, I.; Shapira, A.; Shacham-Diamand, Y.; Dvir, T. Engineered Hybrid Cardiac Patches with Multifunctional Electronics for Online Monitoring and Regulation of Tissue Function. *Nat. Mater.* **2016**, *15* (March), 1–8.

(18) Greiner, A.; Wendorff, J. H. Electrospinning: A Fascinating Method for the Preparation of Ultrathin Fibers. *Angew. Chemie - Int. Ed.* **2007**, *46* (30), 5670–5703.

(19) Sill, T. J.; von Recum, H. A. Electrospinning: Applications in Drug Delivery and Tissue Engineering. *Biomaterials*. 2008, pp 1989–2006.

(20) Delaney, J. T.; Liberski, A. R.; Perelaer, J.; Schubert, U. S. Reactive Inkjet Printing of Calcium Alginate Hydrogel Porogens—a New Strategy to Open-Pore Structured Matrices with Controlled Geometry. *Soft Matter* **2010**, *6* (5), 866.

(21) Annabi, N.; Mithieux, S. M.; Weiss, A. S.; Dehghani, F. The Fabrication of Elastin-Based Hydrogels Using High Pressure CO2. *Biomaterials* **2009**, *30* (1), 1–7.

(22) Liu, S.; Jin, M.; Chen, Y.; Gao, H.; Shi, X.; Cheng, W.; Ren, L.; Wang, Y. High Internal Phase Emulsions Stabilised by Supramolecular Cellulose Nanocrystals and Their Application as Cell-Adhesive Macroporous Hydrogel Monoliths. *J. Mater. Chem. B* **2017**, *5* (14), 2671–2678.

(23) Kumar, A.; Mishra, R.; Reinwald, Y.; Bhat, S. Cryogels: Freezing Unveiled by Thawing.

Mater. Today **2010**, *13* (11), 42–44.

(24) Chan, V.; Zorlutuna, P.; Jeong, J. H.; Kong, H.; Bashir, R. Three-Dimensional Photopatterning of Hydrogels Using Stereolithography for Long-Term Cell Encapsulation. *Lab Chip* **2010**, *10* (16), 2062–2070.

(25) Pham, Q. P.; Sharma, U.; Mikos, A. G. Electrospinning of Polymeric Nanofibers for Tissue Engineering Applications: A Review. *Tissue Eng.* **2006**, *12* (5), 1197–1211.

(26) Atala, S. V. M. & A. 3D Bioprinting of Tissues and Organs. *Nat. Biotechnol.* **2014**, *32* (8), 773–785.

(27) Dalton, P. D.; Klinkhammer, K.; Salber, J.; Klee, D.; Möller, M. Direct in Vitro Electrospinning with Polymer Melts. *Biomacromolecules* **2006**, *7* (3), 686–690.

(28) Townsend-Nicholson, A.; Jayasinghe, S. N. Cell Electrospinning: A Unique Biotechnique for Encapsulating Living Organisms for Generating Active Biological Microthreads/Scaffolds. *Biomacromolecules* **2006**, *7* (12), 3364–3369.

(29) Gensheimer, M.; Becker, M.; Brandis-Heep, A.; Wendorff, J. H.; Thauer, R. K.; Greiner, A. Novel Biohybrid Materials by Electrospinning: Nanofibers of Poly(ethylene Oxide) and Living Bacteria. *Adv. Mater.* **2007**, *19* (18), 2480–2482.

(30) Klein, S.; Kuhn, J.; Avrahami, R.; Tarre, S.; Beliavski, M.; Green, M.; Zussman, E. Encapsulation of Bacterial Cells in Electrospun Microtubes. *Biomacromolecules* **2009**, *10* (7), 1751–1756.

(31) Stankus, J. J.; Guan, J.; Fujimoto, K.; Wagner, W. R. Microintegrating Smooth Muscle Cells

into a Biodegradable, Elastomeric Fiber Matrix. *Biomaterials* **2006**, *27*, 735–744.

(32) Xu, F.; Sheardown, H.; Hoare, T. Reactive Electrospinning of Degradable Poly(oligoethylene Glycol Methacrylate)-Based Nanofibrous Hydrogel Networks. *Chem. Commun.* **2015**, *52*, 23–25.

(33) Smeets, N. M. B.; Bakaic, E.; Patenaude, M.; Hoare, T. Injectable and Tunable Poly(ethylene Glycol) Analogue Hydrogels Based on Poly(oligoethylene Glycol Methacrylate). *Chem. Commun.* **2014**, *50* (25), 3306–3309.

(34) Celebioglu, A.; Yildiz, Z. I.; Uyar, T. Electrospun Crosslinked Poly-Cyclodextrin Nanofibers: Highly Efficient Molecular Filtration Thru Host-Guest Inclusion Complexation. *Sci. Rep.* **2017**, *7* (1), 7369.

(35) Jayasinghe, S. N. Cell Electrospinning: A Novel Tool for Functionalising Fibres{,} Scaffolds and Membranes with Living Cells and Other Advanced Materials for Regenerative Biology and Medicine. *Analyst* **2013**, *138* (8), 2215–2223.

(36) Fatih Canbolat, M.; Tang, C.; Bernacki, S. H.; Pourdeyhimi, B.; Khan, S. Mammalian Cell Viability in Electrospun Composite Nanofiber Structures. *Macromol. Biosci.* **2011**, *11* (10), 1346–1356.

(37) Youn, H.-Y.; McCanna, D. J.; Sivak, J. G.; Jones, L. W. In Vitro Ultraviolet-Induced Damage in Human Corneal, Lens, and Retinal Pigment Epithelial Cells. *Mol. Vis.* **2011**, *17* (January), 237–246.

(38) Smeets, N. M. B.; Bakaic, E.; Patenaude, M.; Hoare, T. Injectable and Tunable

Poly(ethylene Glycol) Analogue Hydrogels Based on Poly(oligoethylene Glycol Methacrylate). *Chem. Commun.* **2014**, *50* (25), 3306–3309.

(39) Lutz, J.-F.; Andrieu, J.; Üzgün, S.; Rudolph, C.; Agarwal, S. Biocompatible, Thermoresponsive, and Biodegradable: Simple Preparation of "All-in-One" Biorelevant Polymers. *Macromolecules* **2007**, *40* (24), 8540–8543.

(40) Deller, R. C.; Vatish, M.; Mitchell, D. A.; Gibson, M. I. Synthetic Polymers Enable Non-Vitreous Cellular Cryopreservation by Reducing Ice Crystal Growth during Thawing. *Nat. Commun.* **2014**, *5*, 3244.

(41) Huang, H.; Zhao, G.; Zhang, Y.; Xu, J.; Toth, T. L.; He, X. Predehydration and Ice Seeding in the Presence of Trehalose Enable Cell Cryopreservation. *ACS Biomater. Sci. Eng.* **2017**, *3* (8), 1758–1768.

(42) Pegg, D. E. Principles of Cryopreservation. *Methods Mol. Biol.* **2007**, *368*, 39–57.

(43) Müller-Plathe, F. Different States of Water in Hydrogels? *Macromolecules* **1998**, *31* (19), 6721–6723.

(44) Tanaka, M.; Hayashi, T.; Morita, S. The Roles of Water Molecules at the Biointerface of Medical Polymers. *Polym J* **2013**, *45* (7), 701–710.

Table of Contents Graphic

A Ready-to-Use and Storage-Stable Nanofibrous Tissue Patch Fabricated in a Single Step via Reactive Electrospinning

Fei Xu †, *Megan Dodd* †, *Heather Sheardown* † *and Todd Hoare* * †